EVALUATION OF THE INFLUENCE OF THE PARTICLE SHAPE ON THE THERMAL PARAMETERS IN A PACKED BED WITH GAS AND LIQUID CO-CURRENT DOWNFLOW

Marcos Flávio Pinto Moreira
Federal University of São Carlos (UFSCar), Department of Chemical Engineering, Rodovia Washington Luiz km 235, 13565-905, P.O. Box 676, São Carlos, São Paulo-Brasil
e-mail: pmfmo@iris.ufscar.br

José Teixeira Freire
Federal University of São Carlos (UFSCar), Department of Chemical Engineering, Rodovia Washington Luiz km 235, 13565-905, P.O. Box 676, São Carlos, São Paulo-Brasil
e-mail: freire@power.ufscar.br

Abstract. In this work the heat transfer in packed beds with co-current gas-liquid downflow is studied. The temperature profiles at the entrance and at the exit of the thermal section are obtained by using ring shape sensors. The influence of the gas flow rate, flow regimes and particle shape on the heat transfer phenomenon is verified by analysing the parameters from the pseudo-homogeneous two-parameter model, assuming a parabolic temperature profile at the entrance of the thermal section. Water and air were used as percolating fluids. The particles are glass spheres, glass cylinders and glass parallelepipeds. The acrylic bed has an inner diameter of 5 cm and a height of 80 cm. The gas flow rate varied from 0 to 0.5 $kg.m^{-2}.s^{-1}$. The effects of the gas flow rate, flow regimes and particle shape on the thermal parameters are verified.

Keywords. *Heat transfer; packed bed; Particle Shape; Flow regimes; Liquid saturation*

1. Introduction

Sudies on the heat transfer in packed beds with gas-liquid co-current downflow have been reported by several authors in the literature due to the wide employment of this configuration in technological applications (Weekman and Myers, 1965; Lamine et al., 1996, etc.). Packed beds are used, for instance, in wastewater treatments as trickling filters, in which oxidation reactions are present (see Iliuta et al., 2002). They are also used in hydrogenation and hydrodesulfurization reactions (Lamine et al., 1996). Since these reactions can be highly exothermic, they need to be controlled in order to avoid that the heat produced either causes damage to the products or deactivates the catalyst (Lamine et al., 1992). A detailed study about the heat transfer phenomenon is necessary to improve the control of these operations. According to literature, several factors can affect the heat transfer in packed beds with gas-liquid co-current downflow, such as the particle diameter for instance. In fact, the packing is a very important factor in defining the hydrodynamic characteristics of a packed bed, such as the observed flow regimes and the liquid saturation (Weekman and Myers, 1965; Satterfield, 1975; Herskowitz and Smith, 1983; Gianetto and Specchia, 1992). The hydrodynamic is expected to affect the thermal behavior (Hashimoto et al., 1976; Matsuura et al., 1979a; Matsuura et al., 1979b; Lamine et al., 1996; Mariani et al., 2001). One of the variables that strongly influences the bed packing is the particle shape. In spite of its importance, the effect of particle shape on heat transfer in packed beds has yet been little investigated. In this work the influence of the particle shape (spheres, cylinders and parallelepipeds) on the thermal parameters of a packed bed is studied, as well as the effects of the flow regimes and gas flow rate on these parameters. The thermal parameters are obtained from the pseudo-homogeneous model to two parameters.

2. Heat transfer model

The most applied formulation for heat transfer in gas-liquid co-current downflow in packed beds is the pseudohomogeneous model, in which a local thermal equilibrium is assumed. The basic equation of the pseudohomogeneous formulation does not include the axial term of the heat transfer, (as assumed by most researchers), and is given by:

$$[GCp_g + LCp_l]\frac{\partial T}{\partial z} = k_r[\frac{1}{r}\frac{\partial}{\partial r}(r\frac{\partial T}{\partial r})] \qquad (1)$$

where G and L are the gas and liquid flow rates, Cp_g e Cp_l are the specific heat capacities of gas and liquid, T is the temperature , r and z are the radial and axial coordinates and k_r is the radial effective thermal conductivity.

In this work the boundary conditions adopted for r=R (bed radius) and z=0 (entrance of the thermal section) are:

$$-k_r\frac{\partial T}{\partial r} = h_w(T_{r=R} - T_W) \qquad (2)$$

$$T = T_o \qquad (3)$$

A symmetry condition is assumed at r=0,

$$\frac{\partial T}{\partial r} = 0 \tag{4}$$

where h_W is the wall heat transfer coefficient, T_W is the temperature on the bed wall, T_o is the temperature at r=0 and z=0.

The solution for the above formulation is given by:

$$\varphi = \frac{T - T_W}{T_o - T_W} = 2\sum_{n=1}^{\infty} \frac{(Bi).J_o(a_n \frac{r}{R})\exp[\frac{-k_r a_n^2 z}{R^2(GCp_g + LCp_l)}]}{[(Bi)^2 + a_n^2]J_o(a_n)} \tag{5}$$

where a_n is obtained from the following equation:

$Bi.J_o(a_n) - a_n.J_1(a_n) = 0$, and the Biot effective number is given by: (6)

$$Bi = h_w R/k_r \tag{7}$$

3. Materials and methods

The particles employed in this study were glass spheres, glass cylinders (5 mm in diameter and 3.4 mm high) and glass parallelepipeds (2.9 mm x 5.3 mm x 5.3 mm). The characteristics of these particles and their packing are presented in Table 1.

Table 1 – Particle characteristics

Particles	d_P (mm) (equivalent diameter	ϕ (sphericity)	ε (average bed porosity)
Spheres	4.4	1	0.37
Cylinders	5.0	0.86	0.32
Parallelepipeds	5.4	0.77	0.31

It must be noted that the spheres, cylinders, and parallelepipeds have the same product of sphericity (ϕ) by equivalent particle diameter (d_p), approximately equal to 4.4×10^{-3} m. The product ϕd_p can be considered as a characteristic dimension of the particle, thus making the comparison among the results physically consistent. The fluids percolating the bed were water and air. A diagram of the experimental apparatus is shown in Figure 1.

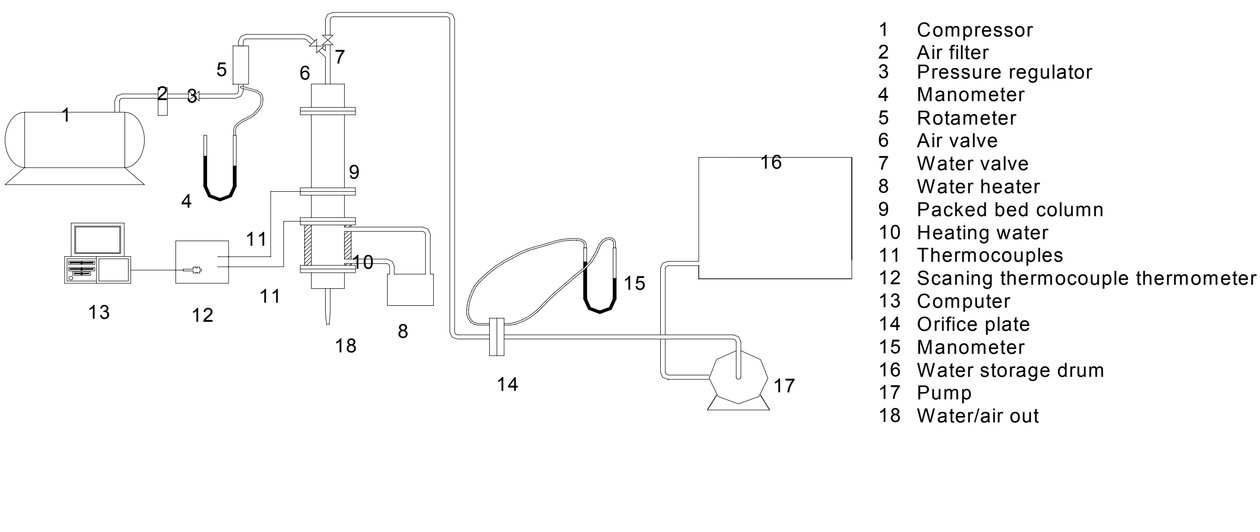

Figure 1. Schematic diagram of the experimental apparatus.

The experimental apparatus was composed of a packed bed with a 50 cm long acrylic column (inner diameter =5 cm), a stainless steel thermal section 20cm long (inner diameter = 5cm) where the tests were performed. The liquid was heated by an electrical heater (8 in Figure 1). The end of the bed was made of a 10cm long acrylic section (inner diameter=5cm) (see Fig. 1).

The water supply consisted of a tank from which the water was pumped to the entrance of the column. Its flow rate was measured with a manometer connected to an orifice plate flowmeter.

The air supply was composed of a compressor, an air filter, a pressure regulator and a rotameter connected to a manometer to measure the air flow rate (see Fig. 1). The fluids were mixed up by a Venturi injector located at the entrance of the bed. Both air and water were discarded after passing through the column.

The packing of particles in the bed was carried out with both air and water flowing. The bed homogeneity was checked by comparing the pressure drops measured in two different sections of the column with water running through it.

The flow regimes were identified visually, at a bed height of about 40-50 cm from the entrance region, at a constant temperature of 25^{o}C.

The dynamic liquid saturation was determined by the drainage method (Rao et al., 1983): the flow was interrupted, the remaining liquid was drained from the bed and the volume of the collected liquid was measured. The residual water (static liquid saturation) was determined by the drying method, which consists in first weighing the moist particles and subsequently drying them in a stove at 105^{o}C until they reach a constant weight. The amount of residual water on the bed's inner wall was neglected. These experiments were also conducted at a constant temperature of 25^{o}C.

For the thermal experiments, fluids entered the bed at a constant temperature of 25^{o}C and the temperature in the thermal section was kept around 45^{o}C with the aid of a water heater (8 in Fig. 1). Initially, only water was supplied to the column at a given water flow rate. Later, Valve 6 was opened and air was supplied to the column. The air flow rates varied from 0 to 0.5 kg.m^{-2}.s^{-1}, the water flow rate (L) was kept at a constant value equal to 20 kg.m^{-2}.s^{-1}.

The temperature profiles were measured using thermocouples at the entrance and at the exit of the thermal section. The electrical signs were converted to digital values (12 in Fig. 1) and transmitted to a computer by a RS-232 interface.

Based on Giudici and Nascimento (1994), ring sensors were used for measuring the temperature in order to filter angular temperature oscillations. Fig. 2 presents these sensors installed between the acrylic and the stainless steel section.

The temperature was measured in 7 radial positions (0, 0.16.R, 0.34.R, 0.48.R, 0.64.R, 0.78.R and 0.94.R) at the entrance and at the exit of the thermal section.

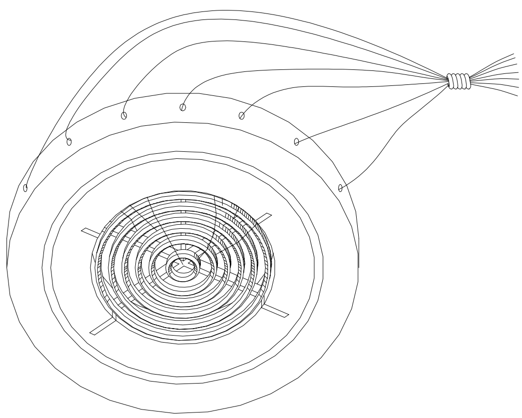

Figure 2. Ring shape sensors.

Steady temperature profiles were used to obtain the thermal parameters.
These thermal parameters were estimated by minimizing a function F trough an optimization method (Marquardt, 1963). Twenty terms were used in Equation (5), a large enough number to obtain the minimum value for F. The a_n's were obtained from Equation (6) by the Regula-Falsi method. Experiments were repeated twice under the same conditions in order to verify their reproducibility.

4. Hydrodynamics

A bubble flow, a transition- I- flow and a pulsed flow regimes were identified for all the packings (spheres, cylinders and parallelepipeds). Details of the experimental procedure are presented in Moreira and Freire (2003). For all the particles, at a water flow rate of 20 kg.m^{-2}.s^{-1}, the presence of a bubble flow regime was observed from G equal to 0.03 to G close to 0.08 kg.m^{-2}.s^{-1}. For air flow rates greater than 0.08 kg.m^{-2}.s^{-1} a transition- I -regime appears and is extended up to G=0.25kg.m^{-2}.s^{-1}. From this rate until G=0.5 kg.m^{-2}.s^{-1} a pulsed flow state is observed. The static liquid saturation was kept at a constant value equal to 0.11 for all the particles tested. The dynamic liquid saturation varied depending on the air flow rate and on the particle shape. Figure 3 presents these experimental results.

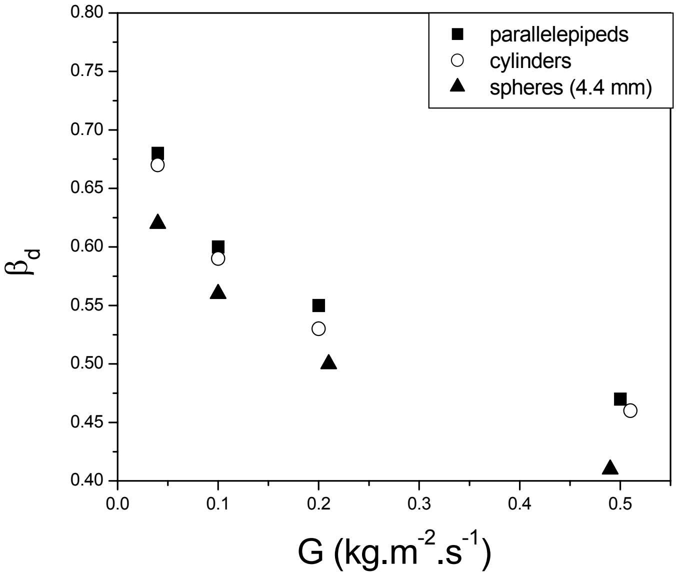

Figure 3. β_d in function of the air flow rate for spheres, cylinders and parallelepipeds.

When the air flow rate is increased, a decrease in the amount of liquid in the bed is observed, as shown in Figure 3, with no dependence on the particle shape.

Concerning the influence of particle shape on β_d, it is verified that the dynamic liquid saturation increases when the sphericity is decreased (considering only the particles used in this work). When the sphericity is reduced, the average bed porosity also decreases, what means that the size of pores have been reduced and become more irregular, thus favoring the retention of liquid within in the bed.

5. Temperature profiles in the bed

The temperature profiles at the entrance of the bed were adjusted to the following equation:

$$\frac{T - T_W}{T_o - T_W} = f(r) = 1 - A\left(\frac{r}{R}\right)^2 \tag{8}$$

where A is a coefficient in the parabolic profile assumed at the entrance of the thermal section.

The temperature profiles at the entrance of the thermal section are parabolic and well represented by Equation 8. Thus, the effects of the air flow rate, flow regimes and particle shape on these profiles are investigated through the variation of parameter A (obtained from equation 8). Figure 4 shows the variation of A as a function of the air flow rate, for different particle shapes and flow regimes.

It is observed that most values of A vary in a range from 0.03 to 0.05, as shown in Fig. 4, and the dependence of A on the air flow rate, flow regimes or particle shape is not well-defined.

At the exit of the thermal section the values of A are observed to be higher than those observed at the bed entrance (meaning more developed parabolic temperature profiles). This is expected because at the bed entrance, the profile is approximately flat but as the fluids enter the thermal section, the temperature profile tends to become parabolic and dependent on the bed length. At $z \to +\infty$, .the profile becomes flat again, because a thermal equilibrium condition is reached.

In this work, the effects of the air flow rate, flow regimes and particle shape on the heat transfer phenomenon are investigated by obtaining the thermal parameters from the pseudo-homogeneous two-parameter model. The fitting between the estimated and measured temperature profiles was satisfactory.

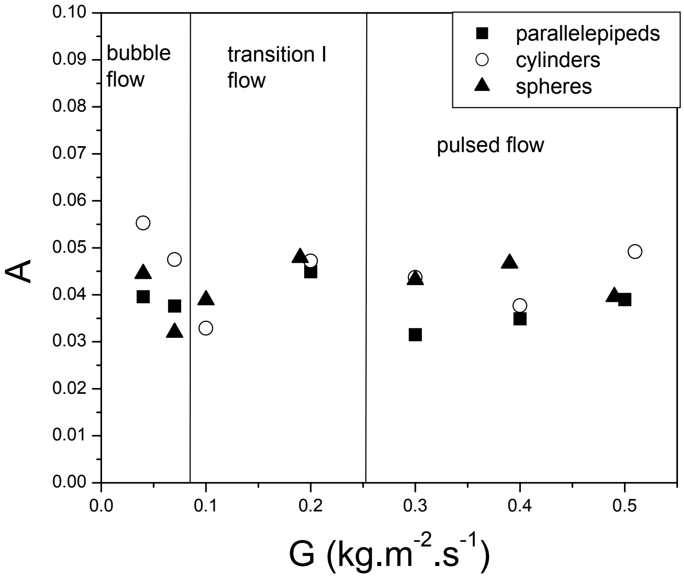

Figure 4. A in function of the air flow rate, flow regime and particle shape.

6. Heat transfer phenomenon

The heat transfer on the bed wall can be analyzed by the wall heat transfer coefficient (h_W). Figure 5 presents the behavior of h_W as a function of the air flow rate, at different flow regimes and particle shapes.

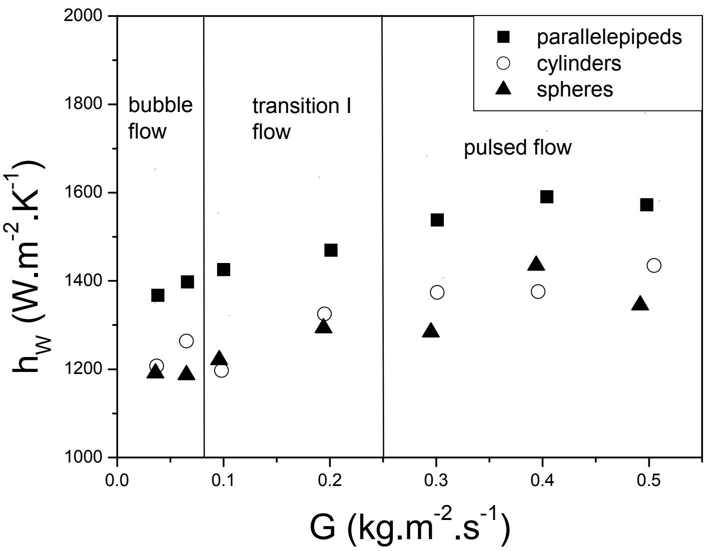

Figure 5. h_P in function of the air flow rate, flow regime and particle shape.

In general, it is noted an increase of h_W when the air flow rate is increased, for all the particles used, from bubble flow to pulsed flow regimes. This occurs because the flow is more disturbed next to the wall as the air velocity is increased.

An increase of h_W also occurs when the particle sphericity is decreased as a result of the increase in the liquid saturation (as described previously, see Fig. 3) and the heat transfer is enhanced due to the higher amount of liquid between particles and wall.

Concerning the radial effective thermal conductivity, Figure 6 presents k_r as a function of the air flow rate, for different flow regimes and particle shapes.

It is observed that the qualitative dependence of k_r on the air flow rate is similar for spheres, cylinders and parallelepipeds. There is a decrease of k_r when the air flow rate is increased and the regimes change from bubble flow to transition I and pulsed flow regimes. Note that according to Figure 6, that near the one-phase waterflow, k_r is greater than those obtained for all the other flow regimes reached in the range of air flow rates investigated (see in Fig. 6 the behavior of k_r for spheres). This indicates that the presence of air in the column is not favoring the radial heat transfer, and the interaction between liquid and gas inside the bed contributes to reduce the heat transfer rates. This assumption is further supported in some studies about heat transfer in packed beds with gas-liquid upflow (Nakamura et al., 1981; Silveira, 1990; Moreira and Freire, 2002), in which the presence of peaks in the curves of k_r versus air flow rate was reported.

It was also observed that k_r is affected by the particle shape. According to Fig. 6, as either the sphericity or the average bed porosity are increased, there is a decrease of k_r. It must be noted that in this study, the increase in the sphericity results in an increase in both the average bed porosity and liquid saturation, causing an increase in the radial heat transfer. The presence of water inside the bed, specifically in the pores in contact with air and particles, enhances the heat transfer due to its high thermal conductivity.

Another point to be considered is the type of contact among the particles inside the bed. As the sphericity is decreased, as occurs for the particles used in this study, the contact area among the packed particles increases, improving the conductive heat transport among them.

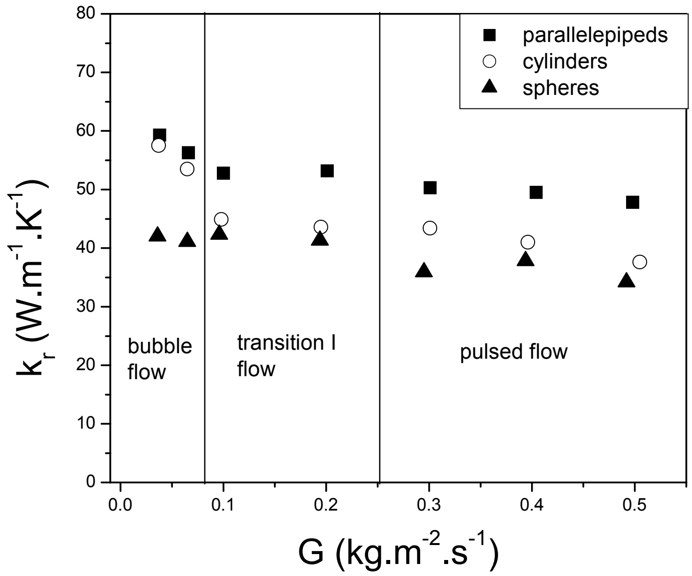

Figure 6. k_r as a function of the air flow rate, flow regimes and particle shapes.

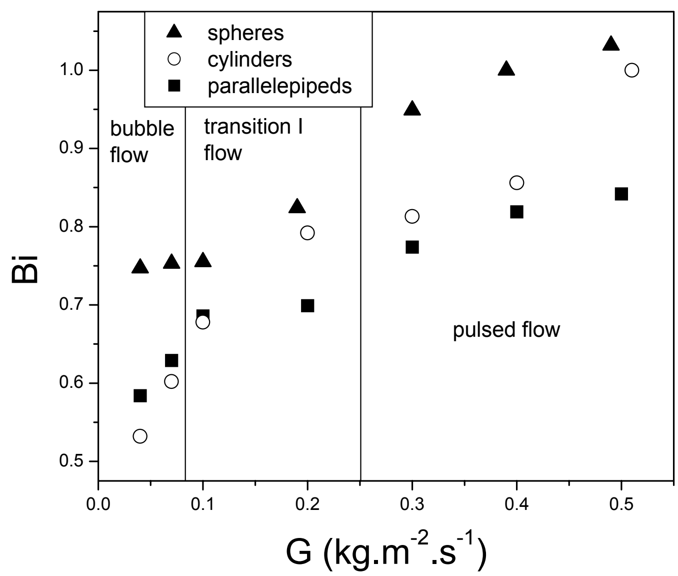

Figure 7. Bi in funtion of the air flow rate, flow regime and particle shape.

The effective Biot number (referred as Bi in this work), represents the ratio between the "effective conductive resistance/effective convective resistance". Its dependence on the air flow rate, as shown in Fig. 7, is expected because h_W increases with increasing the air flow rates. As a result, k_r decreases, thus causing an increase in Bi as the air flow rate is increased (see Equation 7). The particle shape also affects the Bi. An increase in the sphericity causes an increase in Bi.

7. Conclusions

According to this work, the particle shape affects the hydrodynamic characteristics of the gas-liquid co-current downflow through packed beds, as well as the porous media structure, which is represented by the average bed porosity. It was assumed that a possible reduction in the size of pores within the bed occurs as the particle sphericity is decreased, resulting in increasing of the liquid holdup in the column. It seems, although final proof, that the pore shape might have been modified due to the particle shape used in the packing.

All the alterations caused by the particle shape on the structure of the porous media, which affect the hydrodynamic characteristics, affect the thermal characteristics too, as could be observed through the temperature profiles in the thermal section.

To understand the heat transfer phenomenon, the model considered in this work is satisfactory since good fittings have been obtained. The parameter A, which characterize the temperature profile at the entrance of the thermal section, seems to be little affected by the particle shape, air flow rates or flow regimes, while the wall heat transfer coefficient and the radial effective thermal conductivity are affected by these variables. h_W increases either as the air flow rate or the average bed porosity are increased and the sphericity is reduced. k_r increases with decreasing the air flow rates, the average bed porosity and the sphericity.

8. Acknowledgement

We would like to thank the Brazilian funding agencies FAPESP (Fundação de Amparo à Pesquisa do Estado de São Paulo), PRONEX/FINEP (Research and Project Financer) and CNPq (Conselho Nacional de Desenvolvimento Científico e Tecnológico) for their financial assistance.

9. References

Gianetto, A.; Specchia, V., 1992, "Trickle-Bed Reactors: State of Art and Perspectives", Chemical Engineering Science, 47(13-14), pp. 3197-3213.

Giudici, R.; Nascimento, C. A. O., 1994, "Analysis of Ring Shaped Sensor for Use in Packed Bed Heat Transfer Studies", Canadian Journal of Chemical Engineering, Vol.75, pp. 43-49.

Hashimoto, K.; Muroyama, K.; Fujiyoshi, K.; Nagata, S., 1976, " Effective Radial Thermal Conductivity in a Cocurrent Flow of a Gas and Liquid Through a Packed Bed", Int. Chem. Eng., 16(4), pp. 720-727.

Herskowitz, M; Smith, J. M., 1983, "Trickle-Bed Reactors: A Review", A.I.Ch.E. Journal, Vol.29(1), pp. 1-18.

Iliuta, I.; Bildea, S. C.; Iliuta, M. C.; Larachi, F., 2002, "Analysis of Trickle Bed and Packed Bed Bubble Column Bioreactors Form Combined Carbon Oxidation and Nitrification", Brazilian Journal of Chemical Engineering, Vol. 19, No. 1, pp.69-87.

Lamine, A. S., Colli, M. T. and Wild, G., 1992, "Hydrodynamics and Heat Transfer in Packed Bed With Cocurrent Upflow", Chemical Engineering Science, Vol.47, No. 13-14, pp. 3493-3500.

Lamine, A. S., Gerth, L.; Le Gall, H.; Wild, G., 1996, "Heat Transfer in Packed Bed Reactor With Cocurrent Downflow of a Gas and a Liquid" , Chemical Engineering Science, 51(15), pp. 3813-3827.

Mariani, N. J.; Martínez, O. M.; Barreto, G. F., 2001, "Evaluation of Heat Transfer Parameters in Packed Beds With Cocurrent Downflow of Liquid and Gas", Chemical Engineering Science, Vol.56, pp. 5995-6001.

Marquardt, D. W., 1963, "An Algorithm for Least Squares Estimation of Nonlinear Parameters", SIAM – J. Appl. Math., Vol.11, pp. 431-441.

Matsuura, A.; Hitaka, Y.; Akehata, T.; Shirai, T., 1979a, "Effective Radial Thermal Conductivity in Packed Beds with Gas-Liquid Downflow", Heat Transfer – Jap. Res., 8(1), pp. 44-52.

Matsuura, A.; Hitaka, Y.; Akehata, T.; Shirai, T., 1979b, "Apparent Wall Heat Transfer Coefficient in Packed Beds with Downward Cocurrent Gas-Liquid Flow", Heat Transfer – Jap. Res., 8(1), pp. 53-60.

Moreira, M. F. P.; Freire, J. T., 2003, "Influence of Gas and Liquid Flow Rates and the Size and Shape of Particles on the Regime Flow Maps Obtained in Co-current Gas-Liquid Downflow and Upflow Through Packed Beds", Industrial & Engineering Chemistry Research, 42 (4), pp. 929-936.

Moreira, M. F. P.; Freire, J. T., 2003, "Analysis of the Effect of the Particle Shape on the Hydrodynamic and Thermal Behaviors in a Packed Bed with Co-current Gas-Liquid Upflow" (in Portuguese), Proceedings of XXX ENEMP, São Carlos, Brasil (in CD-ROM).

Nakamura, M; Tanahhashi, T.; Takada, D.; Ohsasa, K.; Sugiyama, S., 1981, "Heat Transfer in a Packed Bed with Gas-Liquid Cocurrent Upflow", Heat Transfer - Jap. Res., 10, pp. 92-99.

Rao, V. G.; Ananth, M. S.; Varma, Y. B. G., 1983, "Hydrodynamics of Two-phase Co-current Downflow Through Packed Beds", A.I.Ch.E. Journal, Vol.29, pp. 467-483.

Satterfield, C. N., 1975, “Trickle-Bed Reactors”, A.I.Ch.E. Journal, Vol.21(2), pp. 209-228.
Silveira, A. M, 1991, “Heat Transfer in Porous Media: Analysis of the One-Phase Model in Packed Bed” (in Portuguese), COPPE/UFRJ, Rio de Janeiro, 201 pp. (Thesis).
Weekman, V. W.; Myers, J. E., 1965, “Heat Transfer Characteristics of Co-current Gas-Liquid Flow in Packed Beds”, A.I.Ch.E. Journal, 11(1), pp. 13-17.